



Poiseuille and extensional flow small-angle scattering for developing structure–rheology relationships in soft matter systems

Avanish Bharati^{1,2}, Steven D. Hudson³ and Katie M. Weigandt¹

Abstract

As the rheoscattering community has grown, so has the breadth of experiments both in terms of materials systems, and also in terms of flow types and analysis approaches. In this review, we seek to highlight important recent developments in rheoscattering that go beyond simple shear measurements. In particular, this review will focus on Poiseuille flow and extensional flow small-angle scattering and results from recent experiments that lead to the development of structure–function relationships in a wide variety of soft materials.

Addresses

¹ Center for Neutron Research, National Institute of Standards and Technology, Gaithersburg, USA

² Department of Chemical and Biomolecular Engineering, University of Delaware, Newark, USA

³ Materials Science and Engineering Division, National Institute of Standards and Technology, Gaithersburg, USA

Corresponding author: Weigandt, Katie M (Kathleen.weigandt@nist.gov)

Current Opinion in Colloid & Interface Science 2019, 42:137–146

This review comes from a themed issue on **X-Ray and Neutron Scattering**

Edited by **Jeff Penfold** and **Norman J. Wagner**

For a complete overview see the [Issue](#) and the [Editorial](#)

<https://doi.org/10.1016/j.cocis.2019.07.001>

1359-0294/Published by Elsevier Ltd.

Keywords

Nonlinear deformation, Shear, Poiseuille flow, Capillary rheometer, Slit rheometer, Extensional flow, Mixed flow, Flow-induced structure, RheoSANS, RheoSAXS.

Introduction

Soft material systems are almost exclusively multi-component and/or multiphase and can exhibit hierarchical structures over broad length scales. Soft materials can encounter significant nonlinear flow fields during processing and application, undergoing shear and/or extensional flow with deformation rates that can span decades in magnitude and cause significant structural changes [1]. The relationship between flow and stress governing the rheological properties, either

locally or in bulk, is inextricably linked to the intrinsic structure [2]. Thus, interrogation of structure in soft materials *in situ* under industrially relevant conditions yields valuable insight into material performance and design. Furthermore, validating molecular theories and predictions of nonlinear constitutive rheological models allow probing the underlying molecular processes, especially in less accessed, yet significant, non-linear conditions.

Scattering techniques provide an indispensable tool for probing the structure and dynamics of a broad class of soft matter systems under flow [3]. The underlying principles of scattering are well understood, and the governing interpretations are essentially irrespective of incident radiation. Small-angle scattering (SAS) and wide-angle scattering (WAS) have proven to be extremely useful for *in situ* interrogation of soft matter with length scales varying from a few Å to few μm. The choice of incident radiation depends upon the transient nature of the underlying processes, the complexity of the system under study, sample environment constraints, and the length scale of interest. There are a few key differences to consider when determining which type of scattering experiment is best for specific measurements. In this review, we discuss the experimental literature pertaining to the study of soft matter systems under nonlinear nonsimple flows combined with *in situ* SAS/WAS of neutrons and X-rays. What exactly do we mean by nonsimple flows? For the context of this review, we will discuss nontypical shear rheoSAS methods (capillary and slit flow cells), extensional flows and mixed flows. And by nonlinear, we mean deformations that exceed the small strain limit for linear stress response.

Capillary and slit flow cells both fall under the umbrella of Poiseuille flow or pressure-driven flow through confined geometries [1]. This type of flow field is often encountered in industrial applications where materials are pumped from one part of a process to the next or even in the final delivery or use of a product. From the point of view of SAS experiments, Poiseuille shear flows offer the advantage of the highest accessible shear rates and reduce some of the challenges associated with sliding plate geometries, rotational tool geometries, tool

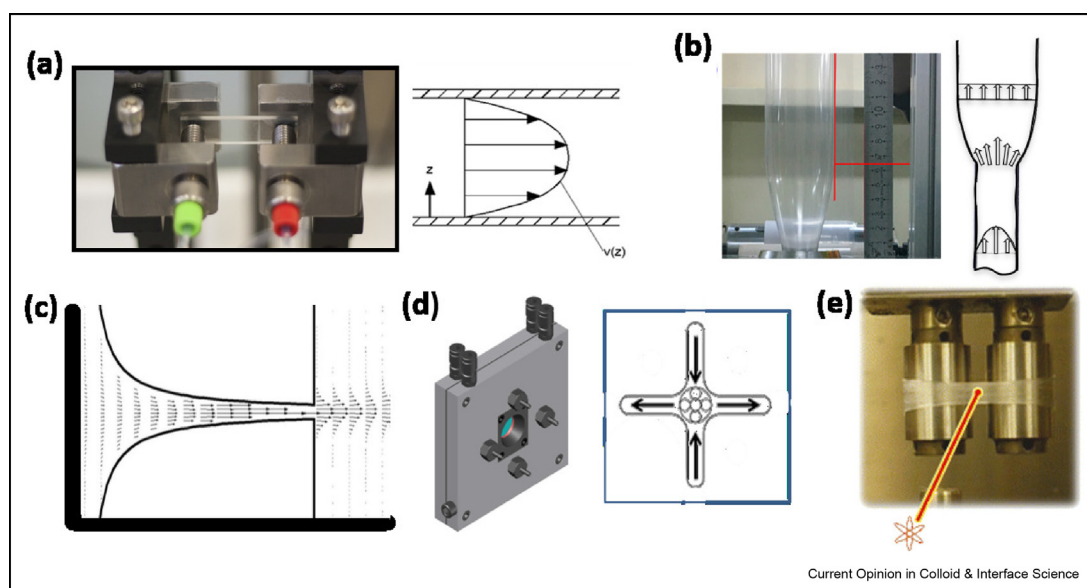
inertia, and sample edge fracture [4]. The main disadvantage of Poiseuille flow for SAS experiments is that there exists a nonuniform stress and shear rate across the sample volume. A slit rheometer for simultaneous neutron and rheology measurements and a cross-sectional view of the streamlines across the height of the slit cell are depicted in Figure 1a. A slit rheometer in combination with SAS/WAS has successfully measured the alignment of worm-like micelles (WLMs) [5–7] as well as flow-induced crystallization of isotactic polypropylene (iPP) [4].

Despite extensive focus on simple shear flows in the literature, mixed shear, extensional, and rotational flows are ubiquitously encountered in real-world situations. In the processing and application of materials, these more complex flows can be observed during contraction or expansion at the entry and exit of pipes or other processing equipment. Some examples of tools used to interrogate mixed and extensional flows include a film-blowing apparatus (Figure 1b) [8], hyperbolic contractions (Figure 1c) [9], cross-slot flow cells (Figure 1d), and extensional rheometers (Figure 1e). Mixed flows often lead to position-dependent flow fields and deformations such that an aperture size that is a small relative to the whole sample volume allows determination of position-dependent structural information. This is particularly useful in the cases of contractions/expansion, die swell, and cross-slot experiments. The effects of mixed shear and extensional deformation on the orientation and anisotropy in liquid crystalline

polymers [10–13], polymer melts [8,14,15], and micelle solutions [16–19] have been thus investigated with various flow SAS techniques.

Planar extensional flows with nonlinear deformations have been achieved at the stagnation points of the cross-slot flow cell and the four-roll mill. The Sentmanat Extensional Rheometer (SER) and other stretching devices are also used to probe uniaxial extensional flow of elastomers and polymers (i.e. materials with more solid-like properties). In Figure 1d, the schematic of a cross-slot for neutron scattering is shown. The stagnation point is located at the center of the middle circle in the schematic. When a small beam passes through or near the stagnation point, the structure at a given extensional strain rate is interrogated. The structure as a function of strain rate can be probed by varying the inlet flow rate. Outside of the stagnation point, the flow field has contributions from shear, rotational, and extensional deformation. SAS in combination with extensional flow cells comprising a cross-slot or a four-roll mill have been used to investigate the extensional flow-induced ordering and alignment at and around the stagnation point of surfactant mixtures [20,21], colloidal suspensions [22–24], and semicrystalline polymers [25]. Alternatively uniaxial extensional deformation can also be probed by stretching samples mounted on various uniaxial stretching apparatus. The experiment is typically designed such that the beam passes through the center of a stretched sample, as shown in Figure 1e. Crystallization, alignment, and other structural changes

Figure 1



Summary of the various sample environments: (a) Flow cell slit rheometer and the schematic of Poiseuille flow across the height of the microchannel, (b) image of bubble (adapted with permission from Ref. [8]) and schematic of the flow field, (c) schematic of the microfluidic hyperbolic contraction flow field (adapted with permission from Ref. [9]), (d) extensional flow cell based on the cross-slot geometry, (e) photograph of the Sentmanat Extensional Rheometer (SER) with a stretched sample and the indication where the neutron beam is centered in the sample (adapted with permission from Ref. [33]).

in polymers have been investigated by combining SAS/WAS with a variety of apparatus including the SER [26–40], a filament stretch–type rheometer (versatile accurate deformation extensional rheometer or VADER) [41–43], or other home-built stretching instruments [44–48].

Poiseuille flows with SAS/WAS

A fully developed Poiseuille flow results in a linear stress profile across the flow cell, such that stress goes from a maximum at the wall to zero at the center-line of the cell. For Newtonian fluids, the velocity profile is, therefore, parabolic. For a Poiseuille flow cell, including slit or capillary rheometers, the viscosity of the material, the pressure limit of the pump, and the design of the flow cell will determine the maximum stress accessible for each measurement. Furthermore, for rheoscattering measurements, the radiation type, scattering volume, beam size, and contrast will determine whether a sample will scatter sufficiently for an experiment to be feasible. That being said, corrections for nonhomogeneous flow fields, various instabilities, viscous heating, wall slip, and compressibility make Poiseuille flow rheometry simple and accurate for most fluids [1,2]. However, for scattering experiments, the beam passes through the entire depth of the flow cell resulting in a depth-averaged and, therefore, stress-averaged scattering data, adding additional complexity to data interpretation. We will discuss here the experimental literature pertaining to the study of soft matter systems subjected to Poiseuille shear flow combined with *in situ* SAS/WAS of neutrons or/and X-rays.

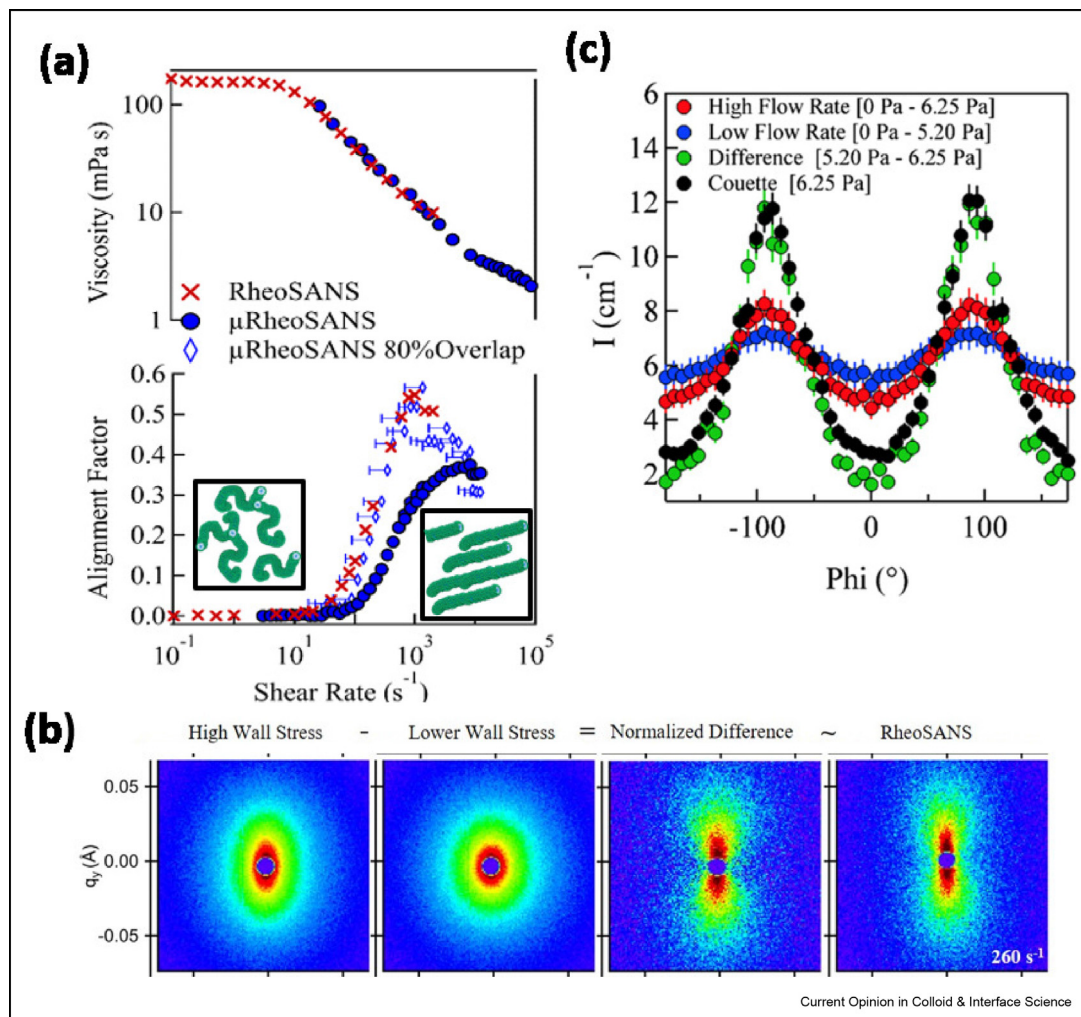
Flow-induced structural changes in polymer and surfactant solutions have been measured in Poiseuille flow cells for years. A variety of capillary, square, and slit cells have been generated for flowSAS measurements. In one example, a polymer–surfactant mixture was studied with both Couette and Poiseuille flow. It was found that the alignment in the Couette flow cell at 5000 s^{-1} was three times the alignment in a Poiseuille flow cell with an equivalent area averaged shear rate [5]. This illustrates an important point. The structure that is probed during a bulk Poiseuille scattering experiment results from the sum of all of the stresses (from zero to wall stress) in the channel and is not well represented by the area average shear rate. Despite this limitation, which has been resolved as discussed below, the average scattering during Poiseuille flow has been used to study a number of soft materials systems to great effect [6]. This is particularly true for polymer melts, which are difficult to study with the Couette tools typically used for traditional rheo-small angle neutron scattering (rheoSANS) measurements. In an example case, the effect of pressure increase due to structure formation during flow-induced crystallization of linear low-density polyethylene in a slit cell was investigated with rheo-

wide and small angle x-ray scattering (WAXS/SAXS) measurements [49]. It was shown that although very short in terms of time, the viscosity rise during flow in confined geometries can have a dominating influence in the crystallization of materials such as polyethylene. In another example case, a portable extruder was designed and constructed for an *in situ* WAXS study on shear-induced crystallization of iPP [50]. By controlling the proportion of the applied axial and circumferential shear field, the orientation of the polymer chains and the final crystal morphology was controlled. A correlation between the external field, chain orientation and conformation, and crystallization was successfully established.

Extracting stress-dependent structural information from Poiseuille flows, where the shear stress and velocity profile change as a function of channel depth, is challenging as the beam samples the material at all of the stress levels existing in the channel. However, so long as the continuum assumption is valid, it can be considered that the stress and, therefore, the structure accumulate additively as the beam propagates through each differential thickness of the sample. This allows for a clever experimental design, where scattering from a sample at a series of wall stresses can be used to deconvolute the stress-dependent scattering [4]. We refer to this approach broadly as a depth sectioning. This approach is valid, provided all other conditions, such as thermal history, material composition, and so on, are held fixed, and it has been used to study polymer crystallization [4] and micellar alignment [7] as a function of stress in various Poiseuille flow experiments.

Real-time, stress-resolved structural information about the development of oriented precursors of iPP was extracted in a pressure-driven slit flow cell [4]. Based on the depth-sectioning approach, information on the orientation distribution of crystallites, the extent of crystallization, and the time at which impingement of crystals occurred was determined and enabled direct correlation of the molecular structure with the macroscopic properties. Recently, the depth-sectioning approach was used to isolate the scattering signal from the high-shear, near-wall region of a semidilute sodium lauryl ether sulfate (SLE-3-S) WLM solution in 8% NaCl brine [7]. The weakly entangled WLMs exhibited typical shear thinning behavior in the steady-flow sweep (Figure 2a) due to shear-induced alignment (inset of Figure 2a). The rheology data from a Couette rheometer and the Poiseuille rheometer, as well as the alignment factor extracted from the simultaneous scattering experiments exhibit good agreement (Figure 2a) and show that, as expected, alignment begins to occur at Weissenberg number (Wi) ≈ 1 . The depth-sectioning approach successfully isolated the scattering from the near-wall, high-stress region of the slit cell (Figure 2b) with a good quantitative agreement between Couette and Poiseuille flow geometries, as illustrated with the

Figure 2



Obtaining scattering and rheology at the wall of a flow-cell. (a) Steady-flow curves as a function of shear rate (wall shear rate for μ RheoSANS measurement) and micelle alignment due to shear-induced alignment (schematics in the inset) from RheoSANS and μ RheoSANS experiments of SLE-3-S micelle solution at 8% NaCl. (b) 2D scattering patterns obtained at $0.009 \text{\AA}^{-1} < q < 0.084 \text{\AA}^{-1}$ of scattering at $260 s^{-1}$. From left to right: scattering patterns of the wall stress followed by $\approx 80\%$ of the wall stress, patterns obtained from using depth-sectioning subtraction technique and measured using Couette RheoSANS at shear rate comparable with the wall shear rates isolated by the subtraction technique. (c) Annular average plot of the scattering intensity for $0.02 \text{\AA}^{-1} < q < 0.03 \text{\AA}^{-1}$ for the scattering pattern shown in (b). Adapted with permission from Ref. [7]. SLE-3-S, sodium lauryl ether sulfate.

annular averaged (Figure 2c for $260 s^{-1}$) and sector averaged plots. Geometry-independent alignment as a function of stress suggested that the anisotropic feature is a shear or stress-induced phenomenon and not the result of flow instability and associated secondary flows.

Mixed and extensional flow with SAS/WAS

Similarly to Poiseuille flow, mixed-flow SAS and extensional-flow SAS measurements offer challenges with respect to isolating stress and flow type-dependent structural changes. For the purpose of this review, we will discuss contraction and expansion flows, including entrance and exit effects, scattering from cross-slots or four-roll mills at and outside of the stagnation point, blow molding apparatus, and stretching devices. A

typical approach for developing stress—structure relationships in these types of measurements is to use a small beam (relative to the flow device) and to measure at a point of pure extensional strain [23] or to create a map of scattering patterns that can be superimposed with a flow field [21] or stress map [51]. This allows for the study of a variety intriguing structural changes including phase changes, alignment, and rheological phenomena including shear thickening or thinning and strain hardening or softening (for liquid-like and solid-like samples, respectively).

Contraction and expansion flow cells

The most similar of these measurements to the Poiseuille flow cell described above are flow through

expansion or contraction experiments. A number of recent studies of WLMs, other micellar systems, and polymer melts have been studied in this manner. An interesting study from the Fischer group used SANS to map the structure of WLM solutions flowing through an abrupt contraction and expansion [16]. *In situ* SANS-mapping revealed that the transient microstructure evolution was contingent on the viscoelasticity, applied rate, position in the flow cell, the degree of the abrupt contraction, and spatial confinement. Highly viscoelastic solutions exhibited pronounced micellar alignment arising from extensional flow at the center line in a slit cell forming a fan-like entry flow at low flow rates.

A similar approach has been taken to study mixtures of bimodal homopolymer blends of two different molar mass. Using selective deuteration the single-chain form factor of the high molecular weight (HMW) component was measured under flow through a 4:1 contraction–expansion flow cell [14]. The use of bimodal blends enabled higher Wi than attained in previous studies on monodisperse melts. Achievement of greater anisotropy in the single-chain form factor was possible in directions both parallel and perpendicular to the flow relative to the center line of the flow cell. Furthermore, a residence time inside the contraction comparable with the terminal relaxation time of the HMW chains allowed the chain anisotropy to persist into the expansion exit region and led to a rapid reversing flow.

In addition to the aforementioned bulk measurements, there has been a recent effort to develop customizable microfluidic devices via soft lithography for microfluidic flowSANS measurements. Several recent articles explore flow-induced micellar growth, lamellar rotation and alignment and changes in orientation, and d-spacing in lamellar sheets [17–19]. In one example, the interplay between lamellar compression and structural relaxation was observed depending on the flow rates and geometry. Large extensional flows resulted in highly oriented lamellar sheets that increased in d-spacing over time [17].

Although not explicitly an expansion–contraction device as discussed previously, an abrupt expansion flow is encountered when the polymer extrudate from a die is blown up to form a bubble during film blowing. Recently, a custom film-blowing device was combined with *in situ* SAXS/WAXS to investigate the structural evolution of a cross-linked polyethylene (PE) bubble along the various zones from the die exit where the structure evolution was similar to that in the processing of biaxial extensional flow fields [8], as shown in Figure 1b. The entangled PE network crystallized into a deformable crystal-crosslinked network upon cooling in the pipe preceding the die exit. This provided sufficient strength to stabilize the bubble (Figure 1b). Similar mixed flow fields were encountered during the stretch-blow molding of biodegradable poly L-lactide. Stretch-

blow molding in combination with X-rays established the connection between deformation, microstructure, and strength to aid the processing of stronger bio-resorbable vascular scaffolds out of the nominally brittle poly L-lactide [15].

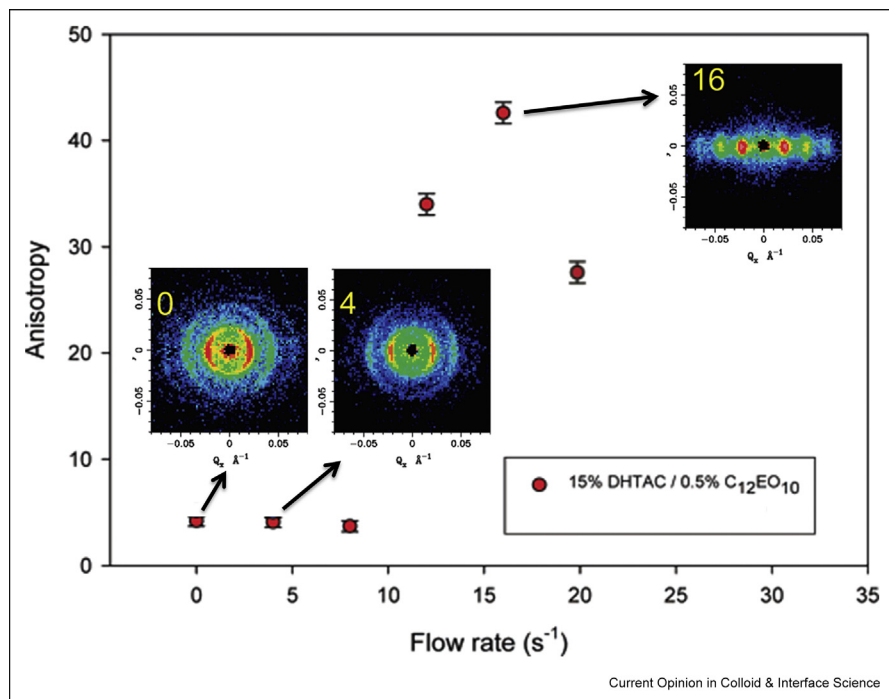
Stagnation point flow cells

Recall from Figure 1d a cross-slot flow cell can be used to generate a stagnation point, which is a point of zero velocity and pure extensional deformation. Similarly, a four-roll mill uses four rotating drums (in an enclosed flow cell) to generate a purely extensional flow at a stagnation point. These devices are useful for studying the effect of nearly pure extensional flows at the stagnation point and mixed flows outside of the stagnation point area for various complex fluids. A cross-slot flow cell developed for SANS measurements by the Penfold group has been used to study charged lamellar micelles as well as mixed microstructures in mixtures of dialkyl chain cationic and nonionic surfactants [20,21]. An abrupt change in the orientation of the lamellae was observed after exceeding the initial alignment threshold, as depicted in Figure 3. The lamellar fragments were significantly aligned in the extensional flow direction at the stagnation point.

In an example of extensional flowSANS of polymer melts, SAXS and WAXS cross-slot studies have been used to study flow-induced crystallization of semi-crystalline polymers [25]. A sharp transition from an amorphous state to the crystalline state was found, and the total final crystallinity increased with increasing strain rate. This suggests that the stretched chain segments should possess some degree of orientation to form flow-induced precursors. It was hypothesized that two competing counter forces, namely van der Waals interactions and entropic force, dominated the formation of oriented precursor structure. As a consequence, if the chain interactions were dominant, the stretched chains formed oriented precursor structures; otherwise, they relaxed.

Cross-slot scattering experiments have also been used to investigate colloidal suspensions [22,24]. More recently, although a fluidic four-roll mill device was developed and used to directly control the flow type (as opposed to mapping different regions of a flow cell) by controlling several inlet flow rates [23]. In combination with SANS, the fluidic four-roll mill was used to probe the direction of orientation and degree of alignment of a semidilute cellulose nanocrystals suspension. Large changes in the orientation distribution of rod-like suspension are predicted in extension dominated flows in the nonlinear regime ($Pe > 1$). However, an accurate interpretation of the local scattering anisotropy was limited by a number of effects including Lagrangian unsteady (i.e., history dependent) responses of the fluid microstructure as

Figure 3



Anisotropy as a function of flow rates for mixtures of dialkyl chain cationic and nonionic surfactants. Insets: Images of scattering intensity at the elongational flow center with flow (extension) rates of 0, 4, 16 s⁻¹. Adapted with permission from Ref. [21].

well as due to large variations in the flow type and deformation rates within the probing neutron beam.

Uniaxial extensional measurements

Uniaxial extensional measurements in the form of film or melt stretching using a variety of experimental apparatus have been adapted for simultaneous scattering studies. These measurements, generally speaking, can be easily distinguished from all of those discussed earlier in the review; in that, the materials under study tend to be limited to soft solids and/or elastomers. This class of measurement is arguably the most active under the umbrella of nonsimple shear rheoSANS measurements owing largely to the ease with which the commercially available rheology tools that hold these soft solids can be adapted to scattering experiments and the time scales over which relevant measurements can be made. In this section, we will discuss the uniaxial stretching of polymers, polymer composites and blends, and elastomeric triblock copolymers.

Nonequilibrium flow-induced crystallization of linear polymers melts [26–31,52] has been extensively investigated by combining *in situ* synchrotron X-ray and step-extension flow generated by SER or home-built twin drum fixtures on a rotational rheometer. Development of stress–structure relationships [53] reveal that

application of critical strain for nucleation in high-density polyethylene [30] combined with a strain rate large enough to overcome the Rouse relaxation results in the onset of stress-upturn accompanied by the formation of thread-like crystalline precursors (shish). Furthermore, flow-induced shish nucleation and growth have proven useful to minimize the true fracture of PE filaments [42,43] and verify the applicability of finite chain extensibility of polystyrene (PS) melts [41] using well-defined steady extensional flows. Flow-induced crystallization studies in combination with *in situ* WAXS during uniaxial extension of poly (ethylene terephthalate) around its glass transition temperature (T_g) illustrated that chain mobility is key to promoting crystallization [46]. In addition, the original orientation of lamellae in the polyethylene oxide (PEO)–sodium iodine composites induced by extensional flow also influenced the crystallization kinetics [34].

The first *in situ* measurements of chain alignment on the length scale of the radius of gyration (R_g) and its correlation with the uniaxial stress state during cold drawing was reported for a linear low-density polyethylene polymer blend of partially deuterated low molecular weight or HMW by combining *in situ* SANS and polarized Raman spectroscopy [36]. The longer chains had a higher probability of connecting at least two crystalline domains across amorphous regions than the shorter chains, whose

characteristic size was postulated to be either $2R_g$ (as a lower limit) or the average end-to-end distance, $h = \sqrt{6}R_g$ (as an upper limit). Flow-induced chain alignment on a series of bi-disperse PS blends during start-up and after cessation of uniaxial extensional flow was performed using SER drums combined with SANS at 150 °C [35]. Transient extensional viscosity during start-up of extensional flow was measured along with the SANS pattern at various extensional strains (Figure 4a). From the annular averaged intensity (Figure 4b), a linear relationship between the alignment factor and the tensile stress for stresses below 65 kPa validated the stress-SANS rule (SSR) in extension (Figure 4c), analogous to the stress-optic rule relating chain alignment to the extensional stress. Recently, uniaxial flow-induced strain hardening was reported for barely entangled poly (4-vinylbiphenyl) melt by combining SER drums with WAXS [54]. Strain hardening was induced by a unique flow-mediated π - π stacking of the phenyl groups and subsequent enhancement of the friction coefficient between polymer chains.

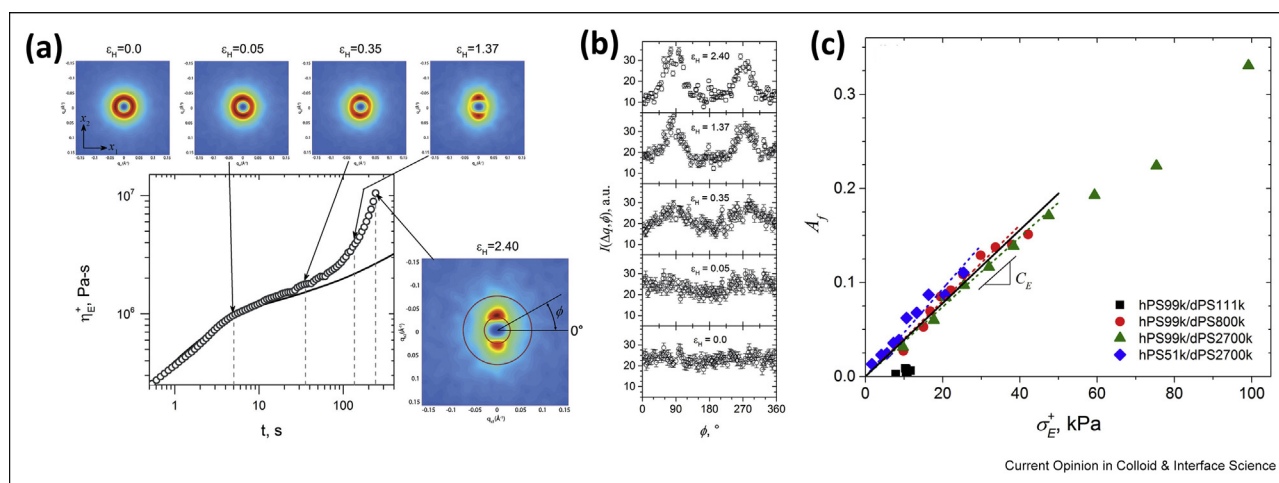
Similar uniaxial extensional measurements have been made to elucidate structural transitions in block copolymer systems including hexagonally ordered cylindrical structures of styrene-ethylene-co-butylene-styrene triblock copolymers using simultaneous time-resolved SAXS [37,40]. Two distinct modes of structural response during extensional flows were observed comprising deformation of the microscopic structure and reorientation of the PS microdomains toward the flow direction [38]. The stress, flow kinematics, and the

microstructural deformation and reorientation were intricately linked with the initial block orientation, being either oriented along or transverse to the flow direction [39]. Furthermore, blends of block copolymers have been similarly investigated: the microstructural origin of the mechanical response of the thermoplastic styrene-isoprene-styrene block copolymer/deuterated PS blends with spherical morphology was studied by combining SANS and SER [33]. Various crystalline phases of deuterated polyethylene/hydrogenated polyethylene blend using SAS were identified in the strain-temperature space [32]. Particularly, the associated changes in the free energy upon imposing flow using twin drums were incorporated in the classical stretched network model to establish the link between temperature and strain. Ultrastretchable ionoelastomers for wearable electronics have been similarly studied: the microstructural origin responsible for the mechanical and electrical properties of self-assembled cross-linked micelles of poly (ethylene oxide)-poly (propylene oxide)-poly (ethylene oxide) (PEO-PPO-PEO) triblock copolymer in a protic ionic liquid was elucidated by combining *in situ* SAXS and uniaxial stretching tool [55–57].

Outlook and future perspectives

Upon application of nonlinear nonsimple shear or extensional flow on soft materials, a strong anisotropy is often generated and easily measured using scattering methods. Traditionally, and as illustrated previously (Figure 4), one method for quantitatively analyzing the anisotropic data is by calculating an alignment factor based on the peaks and troughs in the intensity of the

Figure 4



The stress-SANS rule during the extension of polystyrene. (a) Transient extensional viscosity during start-up of extensional flow (at $\dot{\epsilon} = 0.01 \text{ s}^{-1}$) of hPS99k/dPS2700k blend using the SER. The solid lines were the linear viscoelastic prediction (top) 2D scattering patterns before and during flow start-up corresponding to the indicated extensional strain values. (b) Annular averaged intensity versus azimuthal angle corresponding to the indicated strain values. The averaging was performed using the data corresponding to the ring shown in (a) spanning from 0.025 \AA^{-1} to 0.075 \AA^{-1} . (c) The plot of alignment factor from (a) versus the tensile stress to verify the validity of the stress-SANS rule for various PS blends. Adapted with permission from Ref. [35]. SER, Sentmanat Extensional Rheometer.

scattering relative to the direction of flow. Whether by fitting a Maier Saupe [58] orientation distribution or directly calculating an alignment factor [59], the entire two dimensional—oriented scattering pattern is frequently boiled down to this single parameter and then analyzed with respect to the rheology data. Direct correlation of stress and structure has been referred to as the stress-SANS rule and is analogous to the stress-optical rule for birefringence measurements. It is important to note that accurate interpretation of the scattering anisotropy can be restricted by the unsteady nature of the fluid's microstructure or variations in flow type and deformation rate magnitude within the scattering volume [23]. Moreover, the bulk rheological properties are not necessarily determined by the structural features probed with SAS. For example, in polymer liquid crystals or self-assembled block copolymers, where hierarchical length scales control the rheology, only some of the relevant length scales are accessible with typical SAS measurements.

Recent efforts have sought to move beyond this limited approach. Quantitative metrics from the 2D anisotropic SAS data has been attained by fitting 1D radial sections [60], comparing annular and sector averaged plots [61], fitting isointensity curves [60], and fingerprinting with spherical harmonics [62]. For anisotropic particles at sufficiently low concentration, such that the structure factor is negligible, form factors for anisotropic particles with an orientation distribution can also be fit directly to the 2D scattering data [63,64]. Furthermore, various approximations have been developed to take into account the independent scattering intensity contributions arising from the individual particle, intraparticle, and particle—particle interactions [15,65,66].

The obvious methodology to correlate stress and deformation would be to postulate a molecular theory, predict the SAS spectrum using the modeling framework, and compare it with experiments for a reasonable match. One recent approach is to develop a “fingerprint” with spherical harmonics. Anisotropic pair distribution function in terms of spherical harmonics has successfully shed light on the molecular deformation of soft materials. Spherical harmonic expansion of the orientation distribution function of statistical segments in deformed polymer networks is a viable route to extract information about molecular relaxation at large deformations. This approach offers the advantage of using the entire 2D SANS spectrum; however, as with any analysis approach, care must be taken to ensure that it is applied correctly. It is important to recognize that while the approach is model independent (as it is a parameterization of the scattering data), the theoretical modeling issue remains how stress and other metrics relate to these harmonic coefficients. In one recent example, the spherical harmonic expansion method was combined with a modified network model to extract the

stretch ratio and the radius of gyration of a single chain in a deformed entangled polymer melt [67,68]. Spherical harmonic expansion analysis method may open new avenues for revisiting the existing theoretical frameworks for nonlinear deformations of polymers.

Combining various SAS analysis approaches with molecular modeling to predict the large nonlinear behavior of various soft matter materials will provide a fundamental insight into the validity of various molecular theories developed for finite deformations. This can be achieved by comparing the experimental results with the predictions of constitutive and molecular models. Moreover, the long-standing challenge to quantify the affinity, symmetry, and heterogeneity of macromolecular deformations can be largely addressed. However, going forward, the rheo-scattering community must continue to develop methods to extract more meaningful information from these experiments, particularly for the case of anisotropic particles at relatively high concentrations, where the structure factor contributes significantly to the scattering intensity. As the analysis methods catch up with the wide array of simultaneous scattering and rheology tool kits that exist world wide, we will be able to make unprecedented progress in direct measurement of structure—rheology relationships in a wide variety of soft material systems.

Disclaimer

Certain commercial equipment, instruments, or materials are identified in this article to specify reviewed work adequately. Such identification is not intended to imply recommendation or endorsement by the National Institute of Standards and Technology or to imply that the materials or equipment identified are necessarily the best available for the purpose.

Conflict of interest statement

Nothing declared.

Acknowledgements

Avanish Bharati is supported under cooperative agreement #70NANB15H260 from NIST, U.S. Department of Commerce.

References

Papers of particular interest, published within the period of review, have been highlighted as:

- * of special interest
- ** of outstanding interest

1. [Macosko CW, Larson RG: *Rheology: principles, measurements, and applications*. New York: Vch; 1994.](#)
2. [Morrison F: *Understanding rheology*. Oxford University Press; 2001.](#)
3. [Eberle AP, Porcar L: **Flow-sans and rheo-sans applied to soft matter**. *Curr Opin Colloid Interface Sci* 2012, **17**:33–43.](#)
4. [Fernandez-Ballester L, Thurman DW, Kornfield JA: **Real-time depth sectioning: isolating the effect of stress on structure development in pressure-driven flow**. *J Rheol* 2009, **53**: 1229–1254.](#)

5. Cloke VM, Higgins JS, Phoon CL, Richardson SM, King SM, Done R, Cooper TE: **Poiseuille geometry shear flow apparatus for small-angle scattering experiments.** *Rev Sci Instrum* 1996, **67**:3158–3163.
 6. Castelletto V, Hamley I: **Capillary flow behavior of worm-like micelles studied by small-angle x-ray scattering and small angle light scattering.** *Polym Adv Technol* 2006, **17**:137–144.
 7. Weston JS, Seeman DP, Blair DL, Salipante PF, Hudson SD, Weigandt KM: **Simultaneous slit rheometry and in situ neutron scattering.** *Rheol Acta* 2018, **57**:241–250.
- A Poiseuille slit rheometer was developed and used to interrogate the structure of wormlike micelles at high shear rates. The approach will be useful for extending the ability to develop structure function relationships in complex fluids at shear rates higher than accessible with traditional rheoSAS techniques.
8. Zhang Q, Li L, Su F, Ji Y, Ali S, Zhao H, Meng L, Li L: **From molecular entanglement network to crystal-cross-linked network and crystal scaffold during film blowing of polyethylene: an in situ synchrotron radiation small-and wide-angle x-ray scattering study.** *Macromolecules* 2018, **51**:4350–4362.
- A custom film blowing device for *in situ* SAXS measurements enables measurements that offer unique insight into extensional strain induced structural evolution in polymer melts.
9. Lanzaro A, Li Z, Yuan X-F: **Quantitative characterization of high molecular weight polymer solutions in microfluidic hyperbolic contraction flow.** *Microfluid Nanofluidics* 2015, **18**:819–828.
 10. Bedford BD, Cinader DK, Burghardt WR: **Unstable slit flow of a liquid crystalline polymer solution.** *Rheol Acta* 1997, **36**:384–396.
 11. Burghardt WR, Ugaz VM, Cinader DK: **X-ray scattering measurements of molecular orientation in thermotropic liquid crystalline polymers under flow.** In *ACS symposium series*, vol. 739. American Chemical Society; 1999:374–389.
 12. Burghardt WR, Brown EF, Auad ML, Kornfield JA: **Molecular orientation of a commercial thermotropic liquid crystalline polymer in simple shear and complex flow.** *Rheol Acta* 2005, **44**:446–456.
 13. Vaish N, Cinader Jr D, Burghardt WR, Zhou W, Kornfield J: **Molecular orientation in quenched channel flow of a flow aligning main chain thermotropic liquid crystalline polymer.** *Polymer* 2001, **42**:10147–10153.
 14. Graham RS, Bent J, Clarke N, Hutchings LR, Richards RW, Gough T, Hoyle DM, Harlen OG, Grillo I, Auhl D, *et al.*: **The long-chain dynamics in a model homopolymer blend under strong flow: small-angle neutron scattering and theory.** *Soft Matter* 2009, **5**:2383–2389.
 15. Ramachandran K, Miscioscia R, Filippo G, Pandolfi G, Di Luccio T, Kornfield J: **Tube expansion deformation enables in situ synchrotron x-ray scattering measurements during extensional flow-induced crystallization of poly L-lactide near the glass transition.** *Polymers* 2018, **10**:288.
- An example of how *in situ* X-ray scattering may be used to identify manufacturing process conditions for optimal performance: a connection between deformation, structure, and strength is established during the tube expansion of poly L-lactide.
16. Lutz-Bueno V, Kohlbrecher J, Fischer P: **Micellar solutions in contraction slit-flow: alignment mapped by sans.** *J Non-Newtonian Fluid Mech* 2015, **215**:8–18.
 17. Martin HP, Brooks NJ, Seddon JM, Luckham PF, Terrill NJ, Kowalski AJ, Cabral JT: **Microfluidic processing of concentrated surfactant mixtures: online sans, microscopy and rheology.** *Soft Matter* 2016, **12**:1750–1758.
 18. Lopez CG, Watanabe T, Martel A, Porcar L, Cabral JT: **Microfluidic-sans: flow processing of complex fluids.** *Sci Rep* 2015, **5**:7727.
 19. Lopez CG, Watanabe T, Adamo M, Martel A, Porcar L, Cabral JT: **Microfluidic devices for small-angle neutron scattering.** *J Appl Crystallogr* 2018, **51**:570–583.
 20. Penfold J, Staples E, Tucker I, Carroll P, Clayton I, Cowan J, Lawton G, Amin S, Ferrante A, Ruddock N: **Elongational flow induced ordering in surfactant micelles and mesophases.** *J Phys Chem B* 2006, **110**:1073–1082.
 21. Penfold J, Tucker I: **Flow-induced effects in mixed surfactant mesophases.** *J Phys Chem B* 2007, **111**:9496–9503.
 22. Qazi SJS, Rennie AR, Tucker I, Penfold J, Grillo I: **Alignment of dispersions of plate-like colloidal particles of ni (oh) 2 induced by elongational flow.** *J Phys Chem B* 2011, **115**:3271–3280.
 23. Corona PT, Ruocco N, Weigandt KM, Leal LG, Helgeson ME: **Probing flow-induced nanostructure of complex fluids in arbitrary 2d flows using a fluidic four-roll mill (fform).** *Sci Rep* 2018, **8**:15559.
- The development of the fluidic four roll mill enables scattering based characterization of structural changes in complex fluids that result from rotational, shear, extensional and mixed strain at steady state.
24. Pignon F, Magnin A, Piau J-M, Belina G, Panine P: **Structure and orientation dynamics of sepiolite fibers-poly (ethylene oxide) aqueous suspensions under extensional and shear flow, probed by in situ saxs.** *Rheol Acta* 2009, **48**:563–578.
 25. Keum JK: *Probing flow-induced crystallization precursor structure in polyolefin melts by means of synchrotron x-rays.* Ph.D. thesis. Stony Brook, NY: The Graduate School, Stony Brook University; 2007.
 26. Liu Y, Zhou W, Cui K, Tian N, Wang X, Liu L, Li L, Zhou Y: **Extensional rheometer for in situ x-ray scattering study on flow-induced crystallization of polymer.** *Rev Sci Instrum* 2011, **82**, 045104.
 27. Tian N, Zhou W, Cui K, Liu Y, Fang Y, Wang X, Liu L, Li L: **Extension flow induced crystallization of poly(ethylene oxide).** *Macromolecules* 2011, **44**:7704–7712.
 28. Ju J, Wang Z, Su F, Ji Y, Yang H, Chang J, Ali S, Li X, Li L: **Extensional flow-induced dynamic phase transitions in isotactic polypropylene.** *Macromol Rapid Commun* 2016, **37**:1441–1445.
 29. Wang Z, Ju J, Yang J, Ma Z, Liu D, Cui K, Yang H, Chang J, Huang N, Li L: **The non-equilibrium phase diagrams of flow-induced crystallization and melting of polyethylene.** *Sci Rep* 2016, **6**:32968.
 30. Yan T, Zhao B, Cong Y, Fang Y, Cheng S, Li L, Pan G, Wang Z, Li X, Bian F: **Critical strain for shish-kebab formation.** *Macromolecules* 2009, **43**:602–605.
 31. Yang H, Liu D, Ju J, Li J, Wang Z, Yan G, Ji Y, Zhang W, Sun G, Li L: **Chain deformation on the formation of shish nuclei under extension flow: an in situ sans and saxs study.** *Macromolecules* 2016, **49**:9080–9088.
 32. Liu D, Tian N, Huang N, Cui K, Wang Z, Hu T, Yang H, Li X, Li L: **Extension-induced nucleation under near-equilibrium conditions: the mechanism on the transition from point nucleus to shish.** *Macromolecules* 2014, **47**:6813–6823.
 33. López-Barrón CR, Eberle AP, Yakovlev S, Bons A-J: **Structural origins of mechanical properties and hysteresis in sis triblock copolymers/polystyrene blends with spherical morphology.** *Rheol Acta* 2016, **55**:103–116.
 34. Hu T, Tian N, Ali S, Wang Z, Chang J, Huang N, Li L: **Polymer-ion interaction weakens the strain-rate dependence of extension-induced crystallization for poly (ethylene oxide).** *Langmuir* 2016, **32**:2117–2126.
 35. López-Barrón CR, Zeng Y, Richards JJ: **Chain stretching and recoiling during startup and cessation of extensional flow of bidisperse polystyrene blends.** *J Rheol* 2017, **61**:697–710.
- SANS in combination with *in situ* SER measurements enabled direct correlation of extensional stress and flow-induced chain alignment of polystyrene melts during the startup of uniaxial extension and after cessation of flow, consistent with the validity of the stress-SANS rule.
36. López-Barrón CR, Zeng Y, Schaefer JJ, Eberle AP, Lodge TP, Bates FS: **Molecular alignment in polyethylene during cold drawing using in-situ sans and Raman spectroscopy.** *Macromolecules* 2017, **50**:3627–3636.
- Chain alignment of a semi-crystalline low-density polyethylene polymer was measured with SANS and polarized Raman spectroscopy during cold drawing on a Linkam tensile stage.

37. McCready EM, Burghardt WR: **In situ saxs studies of structural relaxation of an ordered block copolymer melt following cessation of uniaxial extensional flow.** *Macromolecules* 2014, **48**:264–271.
38. Mao R, McCready EM, Burghardt WR: **Structural response of an ordered block copolymer melt to uniaxial extensional flow.** *Soft Matter* 2014, **10**:6198–6207.
39. McCready EM, Burghardt WR: **Structural response of a prealigned cylindrical block copolymer melt to extensional flow.** *J Rheol* 2015, **59**:935–956.
40. Tomita S, Wataoka I, Igarashi N, Shimizu N, Takagi H, Sasaki S, Sakurai S: **Strain-induced deformation of glassy spherical microdomains in elastomeric triblock copolymer films: time-resolved 2d-saxs measurements under stretched state.** *Macromolecules* 2017, **50**:3404–3410.
- The strain-induced deformation and subsequent relaxation of elastomeric triblock copolymers after application of a step strain was studied with time-resolved SAXS. A strong correlation of glassy domain deformation during stress relaxation and the subsequent film fracture is established.
41. Hassager O, Mortensen K, Bach A, Almdal K, Rasmussen HK, Pyckhout-Hintzen W: **Stress and neutron scattering measurements on linear polymer melts undergoing steady elongational flow.** *Rheol Acta* 2012, **51**:385–394.
42. Wingstrand SL, Hassager O, Parisi D, Borger AL, Mortensen K: **Flow induced crystallization prevents melt fracture of hdpe in uniaxial extensional flow.** *J Rheol* 2018, **62**:1051–1060.
43. Wingstrand SL, van Drongelen M, Mortensen K, Graham RS, Huang Q, Hassager O: **Influence of extensional stress overshoot on crystallization of ldpe.** *Macromolecules* 2017, **50**:1134–1140.
- Quenching polymer melts during uniaxial deformation in a filament stretch rheometer enables *ex situ* characterization of polymer structure using SAXS (and could be extended to SANS or other characterization methods).
44. Meng L, Li J, Cui K, Chen X, Lin Y, Xu J, Li L: **A simple constrained uniaxial tensile apparatus for in situ investigation of film stretching processing.** *Rev Sci Instrum* 2013, **84**:115104.
45. Ma Z, Balzano L, Portale G, Peters GW: **Flow induced crystallization in isotactic polypropylene during and after flow.** *Polymer* 2014, **55**:6140–6151.
46. Zhang W, Yan Q, Ye K, Zhang Q, Chen W, Meng L, Chen X, Wang D, Li L: **The effect of water absorption on stretch-induced crystallization of poly (ethylene terephthalate): an in-situ synchrotron radiation wide angle x-ray scattering study.** *Polymer* 2019, **162**:91–99.
- In situ* WAXS measurements on stretched poly (ethylene terephthalate) elucidates that chain stretch and orientation during uniaxial deformation play key roles in stretch-induced crystallization.
47. Niu B, Chen J-B, Chen J, Ji X, Zhong G-J, Li Z-M: **Crystallization of linear low density polyethylene on an in situ oriented isotactic polypropylene substrate manipulated by an extensional flow field.** *CrysiEngComm* 2016, **18**:77–91.
48. Ruocco N, Auhl D, Bailly C, Lindner P, Pyckhout-Hintzen W, Wischniewski A, Leal L, Hadjichristidis N, Richter D: **Branch point withdrawal in elongational startup flow by time-resolved small angle neutron scattering.** *Macromolecules* 2016, **49**:4330–4339.
49. Troisi E, Portale G, Ma Z, van Drongelen M, Hermida-Merino D, Peters G: **Unusual melting behavior in flow induced crystallization of lldpe: effect of pressure.** *Macromolecules* 2015, **48**:2551–2560.
50. Chang J, Wang Z, Tang X, Tian F, Ye K, Li L: **A portable extruder for in situ wide angle x-ray scattering study on multi-dimensional flow field induced crystallization of polymer.** *Rev Sci Instrum* 2018, **89**:025101.
- Use of a portable extruder in combination with *in situ* WAXS gives insight into multi-dimensional flow field induced crystallization of polypropylene. Correlation between chain orientation, conformation, and crystallization is established.
51. Cui K, Liu D, Ji Y, Huang N, Ma Z, Wang Z, Lv F, Yang H, Li L: **Nonequilibrium nature of flow-induced nucleation in isotactic polypropylene.** *Macromolecules* 2015, **48**:694–699.
52. Coppola S, Grizzuti N, Maffettone PL: **Microrheological modeling of flow-induced crystallization.** *Macromolecules* 2001, **34**:5030–5036.
53. Bent J, Hutchings L, Richards R, Gough T, Spares R, Coates P, Grillo I, Harlen O, Read D, Graham R, Likhtman A: **Neutron-mapping polymer flow: scattering, flow visualization, and molecular theory.** *Science* 2003, **301**:1691–1695.
54. López-Barrón CR, Zhou H: **Extensional strain hardening induced by π - π interactions in barely entangled polymer chains: the curious case of poly (4-vinylbiphenyl).** *Phys Rev Lett* 2017, **119**:247801.
55. López-Barrón CR, Chen R, Wagner NJ: **Ultrastretchable iono-elastomers with mechano-electrical response.** *ACS Macro Lett* 2016, **5**:1332–1338.
56. Xie Y, Xie R, Yang H-C, Chen Z, Hou J, López-Barrón CR, Wagner NJ, Gao K-Z: **Iono-elastomer-based wearable strain sensor with real-time thermomechanical dual response.** *ACS Appl Mater Interfaces* 2018, **10**:32435–32443.
57. Xie R, Xie Y, López-Barrón CR, Gao K-Z, Wagner NJ: **Ultra-stretchable conductive iono-elastomer and motion strain sensor system developed therefrom.** *Technol Innov* 2018, **19**:613–626.
58. Maier W, Saupe A: **Eine einfache molekular-statistische theorie der nematischen kristallinflüssigen phase. teil I1.** *Z Naturforschung A* 1959, **14**:882–889.
59. Walker LM, Wagner NJ: **Sans analysis of the molecular order in poly (γ -benzyl l-glutamate)/deuterated dimethylformamide (pblg/d-dmf) under shear and during relaxation.** *Macromolecules* 1996, **29**:2298–2301.
60. Muller R, Pesce J, Picot C: **Chain conformation in sheared polymer melts as revealed by sans.** *Macromolecules* 1993, **26**:4356–4362.
61. Yearley EJ, Sasa LA, Welch CF, Taylor MA, Kupcho KM, Gilbertson RD, Hjelm RP: **The Couette configuration of the los alamos neutron science center neutron rheometer for the investigation of polymers in the bulk via small-angle neutron scattering.** *Rev Sci Instrum* 2010, **81**:045109.
62. Wang Z, Lam CN, Chen W-R, Wang W, Liu J, Liu Y, Porcar L, Stanley CB, Zhao Z, Hong K, et al.: **Fingerprinting molecular relaxation in deformed polymers.** *Phys Rev X* 2017, **7**:031003.
- Formulation of a general mathematical framework is used to parameterize 2D anisotropic scattering data for the purpose here of tracking polymer relaxation.
63. Weigandt KM, Pozzo DC, Porcar L: **Structure of high density fibrin networks probed with neutron scattering and rheology.** *Soft Matter* 2009, **5**:4321–4330.
64. Alina G, Butler P, Cho J, Doucet M, Kienzle P: **Sasview for small angle scattering analysis.** 2017. <http://www.sasview.org>.
65. Hansen S: **Approximation of the structure factor for nonspherical hard bodies using polydisperse spheres.** *J Appl Crystallogr* 2013, **46**:1008–1016.
66. Greene DG, Ferraro DV, Lenhoff AM, Wagner NJ: **A critical examination of the decoupling approximation for small-angle scattering from hard ellipsoids of revolution.** *J Appl Crystallogr* 2016, **49**:1734–1739.
67. Wang Z-Y, Kong D, Yang L, Ma H, Su F, Ito K, Liu Y, Wang X, Wang Z: **Analysis of small-angle neutron scattering spectra from deformed polymers with the spherical harmonic expansion method and a network model.** *Macromolecules* 2018, **51**:9011–9018.
68. Lam CN, Xu W-S, Chen W-R, Wang Z, Stanley CB, Carrillo J-MY, Uhrig D, Wang W, Hong K, Liu Y, et al.: **Scaling behavior of anisotropic relaxation in deformed polymers.** *Phys Rev Lett* 2018, **121**:117801.